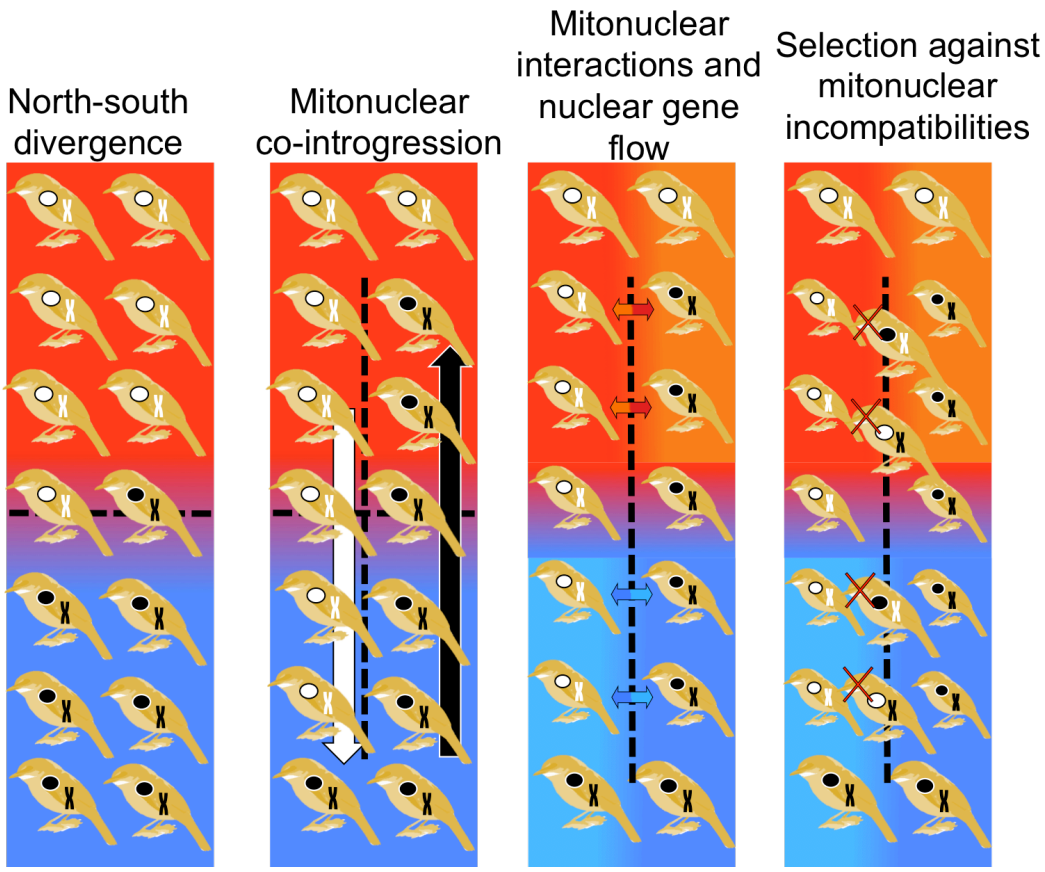

Figure S1 Eastern Yellow Robin (EYR) hypothesized evolutionary history. The colour of the boxes represents birds' nuclear genomic background (north = red and south = blue). Inside of the bird's diagrams, the circle represent mitochondrial DNA (mito-A = white and mito-B = black) and the chromosomes represent nuclear-encoded genes with mitochondrial function (N-mt genes), matching colours represent mitonuclear interactions. The first panel shows the initial differentiation with gene flow between northern and southern birds (Morales *et al.* 2016). The second panel shows two independent events of mitonuclear co-introgression resulting in inland-coastal divergence (Morales *et al.*, 2016; see Results in main text). The third panel shows the maintenance of mitonuclear interactions despite ongoing nuclear gene flow (shades of red and blue differing horizontally highlight the subtle genome-wide differentiation of each genomic background; see Fig. 1B of main text). The fourth panel shows selection against mitonuclear incompatibilities in the inland-coastal hybrid zone (see Fig. 2A of main text). The processes described by the last two panels can occur simultaneously.

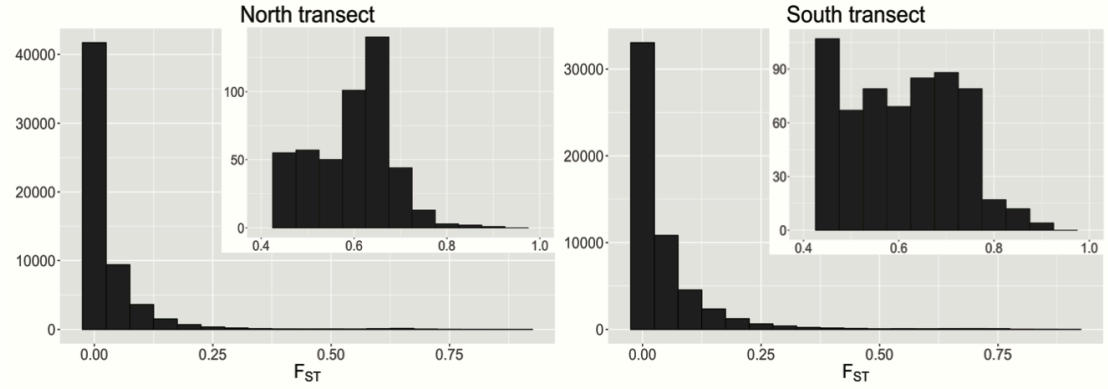

Figure S2 F_{ST} histograms for the analysis at fine spatial scales (including only individuals sampled within 40 km of the centre of the contact zone). The insets show the right tails of the distributions (F_{ST} > 0.4) showing high peaks that are barely visible on the plots with all markers.

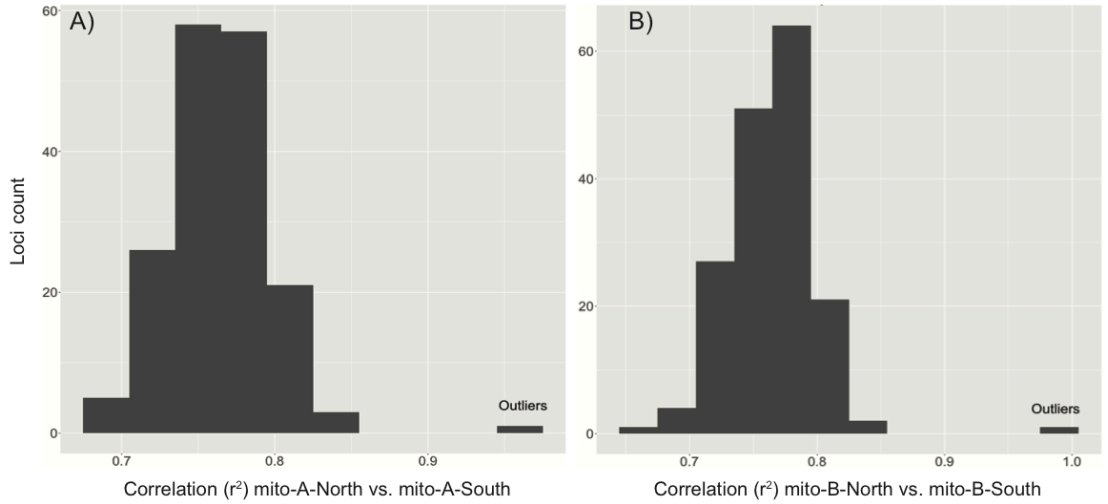

Figure S3 Allelic frequency correlations between north and south transects for outlier and non-outlier loci. (A) Allelic frequency correlation between north mito-A and south mito-A. (B) Allelic frequency correlation between north mito-B and south mito-B. Correlations of outlier loci are significantly higher than expected at random (P<0.001) showing that alleles within mitogroups segregate in the same direction in both nuclear backgrounds. The genomic random distribution was obtained by calculating allelic frequency correlations of 140 sets of non-outlier loci.

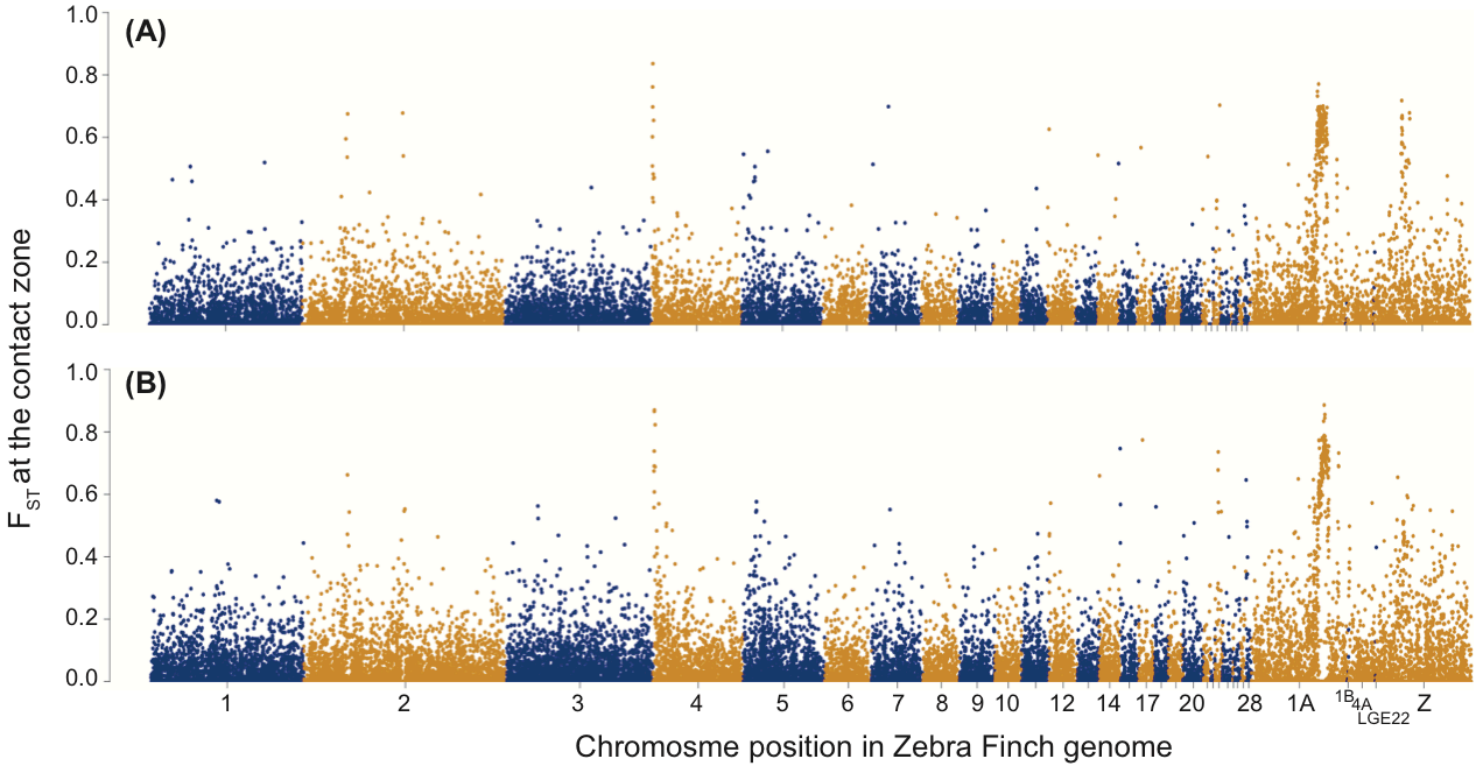

Figure S4 Fine spatial scale F_{ST} analyses. Nuclear DNA differentiation between mitogroups mapped onto the Zebra Finch reference genome for individuals located within a 40-km radius from the midpoint of the contact zone between the two mitolineages in each transect. (A) Northern transect; (B) southern transect; genomic position of each Single Nucleotide Polymorphism as mapped to the Zebra Finch genome is shown on the x-axis; F_{ST} is presented on the y-axis.

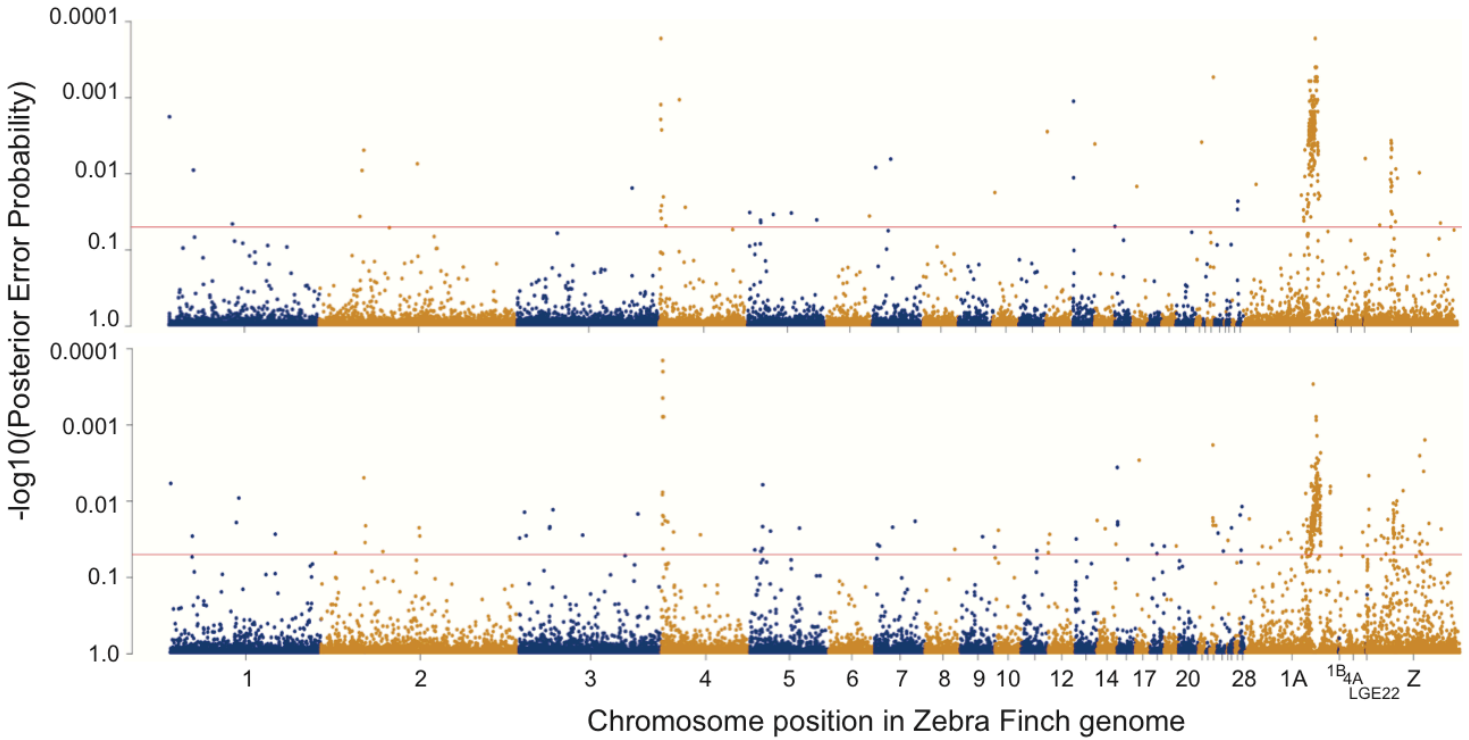

Figure S5 BayScEnv analyses with mitochondrial membership. Nuclear DNA differentiation between populations correlated with a binomial variable of mitolineage membership mapped onto the reference genome for all individuals across each transect. (A) Northern transect; (B) southern transect. The genomic position of each Single Nucleotide Polymorphism as mapped to the Zebra Finch genome is shown on the x-axis. The significance values (see Methods in main text) are depicted in the y-axis, with the False Discovery Rate threshold of 5% shown with a horizontal red line.

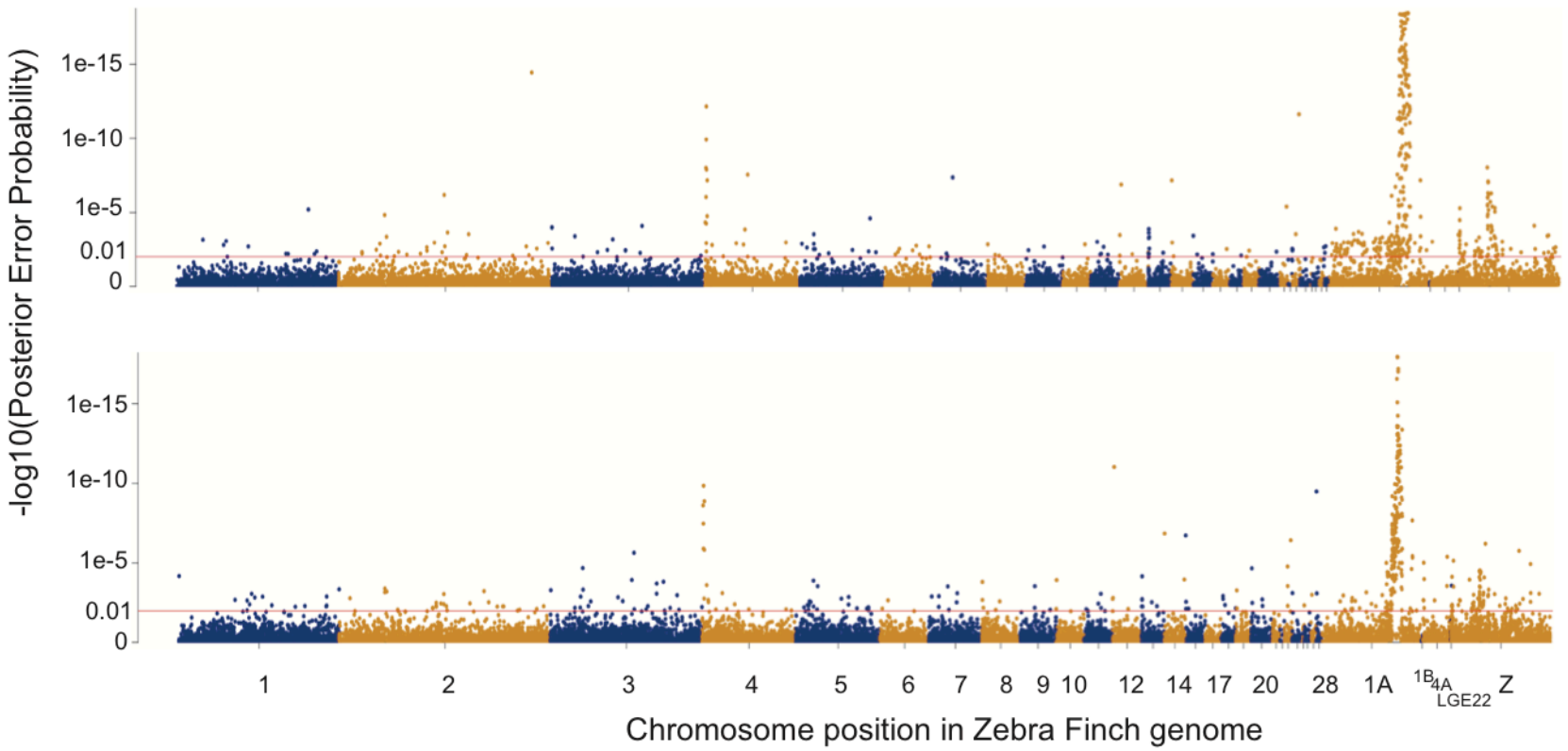

Figure S6 PCAdapt analyses. Nuclear DNA differentiation along the first axis of differentiation (K = 1, see methods) for all individuals across each transect. (A) Northern transect; (B) southern transect. The genomic position of each Single Nucleotide Polymorphism as mapped to the Zebra Finch genome is shown on the x-axis. The significance values (see Methods in main text) are depicted in the y-axis, with the False Discovery Rate threshold of 1% shown with a horizontal red line.

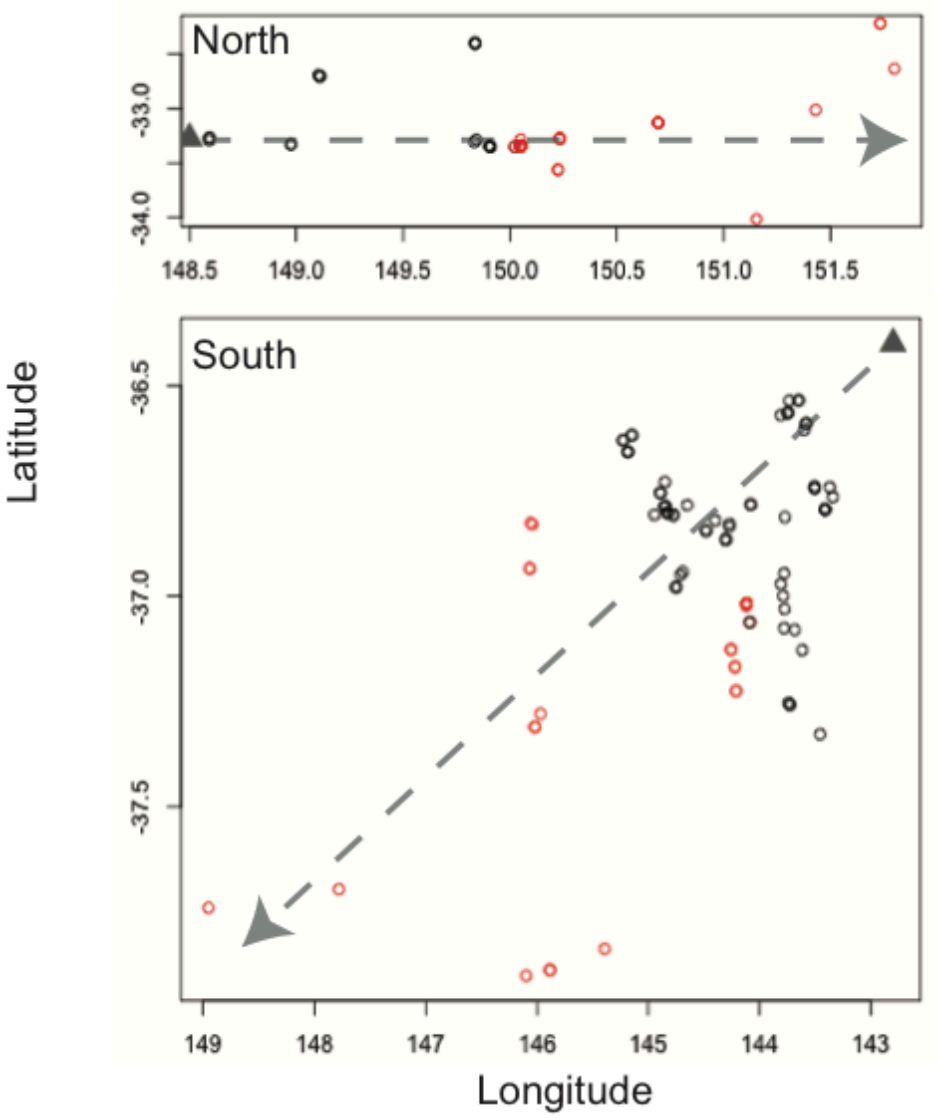

Figure S7 Geographic coordinates of individual samples used in geographic cline analyses. For each transect, we projected the location of each individual sample along a unidimensional transect (dashed line) and calculated the distance of each sample to a common geographic point (triangle). The spread of the samples along the perpendicular axis to the mitochondrial variation (black = mito-A and red = mito-B) likely produces a poor fit of geographic clines, particularly in the south transects. This is likely the reason why the confidence intervals of nuclear clines were so wide (see Results).

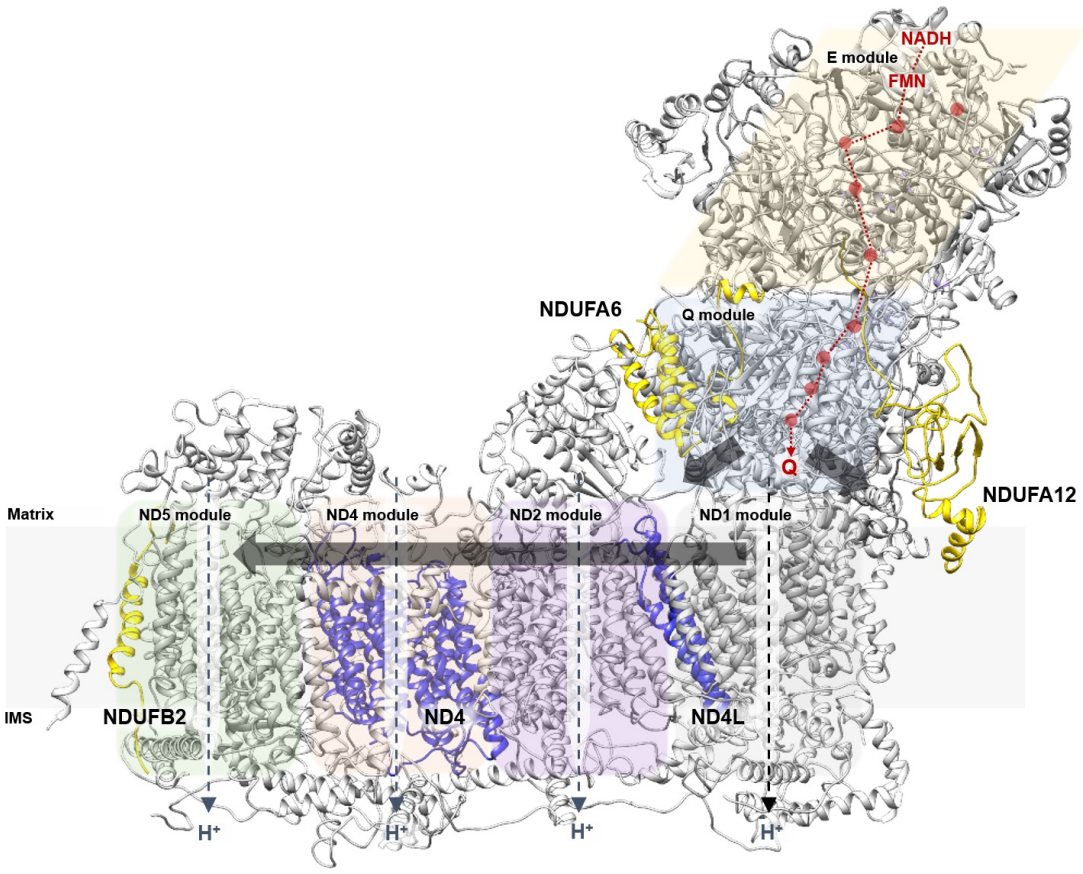

Figure S8 Candidate genes for mitochondrial-nuclear interactions in the Eastern Yellow Robin (EYR) mapped to a three-dimensional model of OXPHOS complex I. Mitonuclear interaction are formed by mitochondrial-encoded genes (mtDNA) and nuclear-encoded genes with mitochondrial function (N-mt). The underlying structure represents the complete structure of the bovine mitochondrial complex I (Zhu *et al.* 2016). The modules responsible for NADH oxidation (E module), ubiquinone reduction (Q module), and proton pumping (ND1, ND2, ND4, and ND5 modules) have differentially shaded backgrounds. Arrows show the routes of electron transfer (thin, dotted, maroon), proton translocation (medium, dashed, navy), and the conformational changes that couple them (thick, solid, grey). EYR N-mt genes in the genomic island of divergence of chromosome 1A (NDUFA6, NDUFA12, NDUFB2; see Fig. 3 of main text) are mapped onto the protein structure (highlighted in yellow). EYR mitochondrially-encoded core subunits that show evidence of positive selection between the mito-A and mito-B are highlighted in purple.

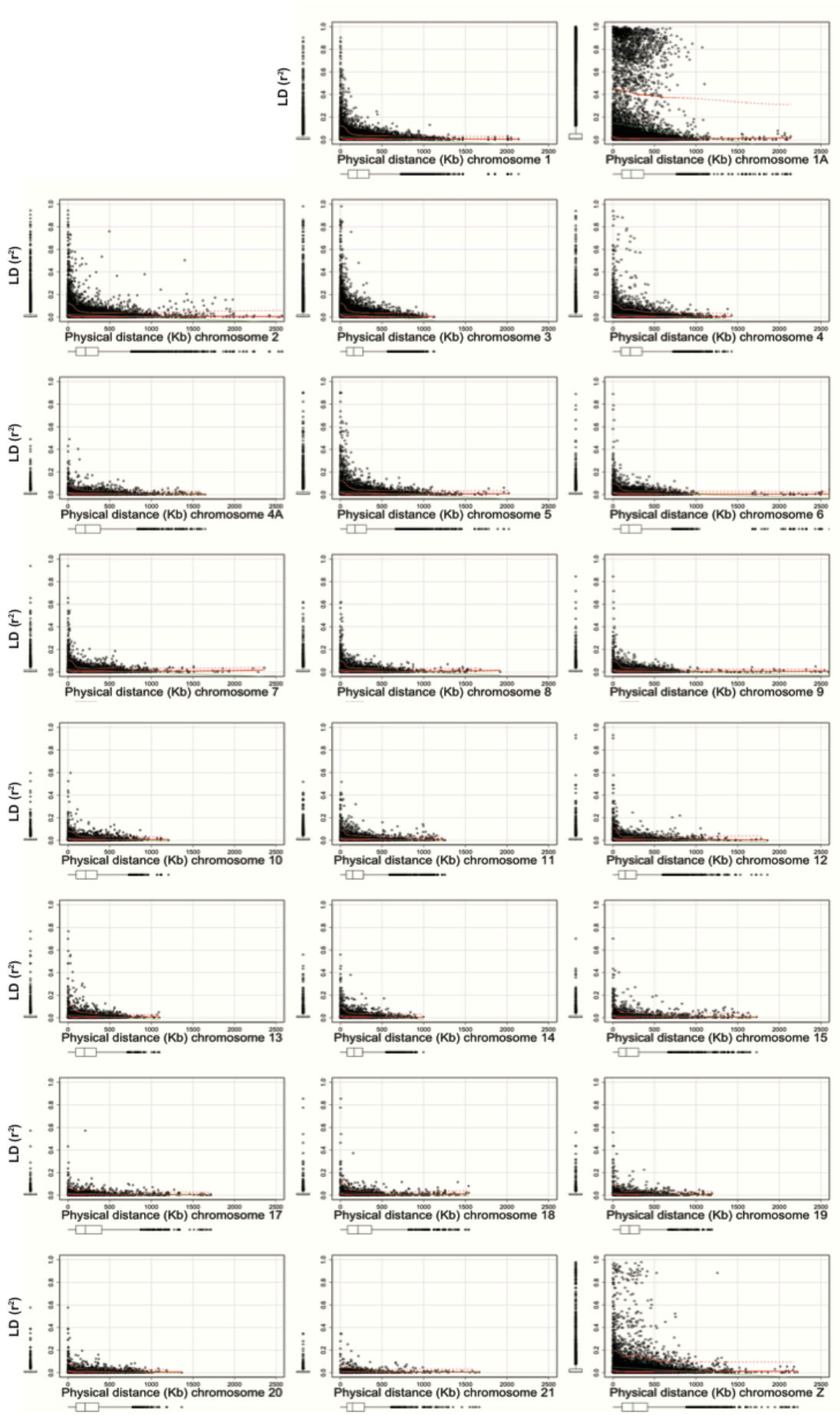
LD (r²)
Physical distance (Kb) chromosome 1
Physical distance (Kb) chromosome 1A
Physical distance (Kb) chromosome 2
Physical distance (Kb) chromosome 3
Physical distance (Kb) chromosome 4
Physical distance (Kb) chromosome 4A
Physical distance (Kb) chromosome 5
Physical distance (Kb) chromosome 6
Physical distance (Kb) chromosome 7
Physical distance (Kb) chromosome 8
Physical distance (Kb) chromosome 9
Physical distance (Kb) chromosome 10
Physical distance (Kb) chromosome 11
Physical distance (Kb) chromosome 12
Physical distance (Kb) chromosome 13
Physical distance (Kb) chromosome 14
Physical distance (Kb) chromosome 15
Physical distance (Kb) chromosome 17
Physical distance (Kb) chromosome 18
Physical distance (Kb) chromosome 19
Physical distance (Kb) chromosome 20
Physical distance (Kb) chromosome 21
Physical distance (Kb) chromosome Z

Figure S9 Plot of linkage disequilibrium (LD, r^2) against physical distance between pairs of loci on Zebra Finch genome, for each chromosome. Black dots indicate observed pairwise LD. Green lines show the expected average decay of LD per chromosome with confidence intervals in red, estimated with a non-linear regression of r^2.

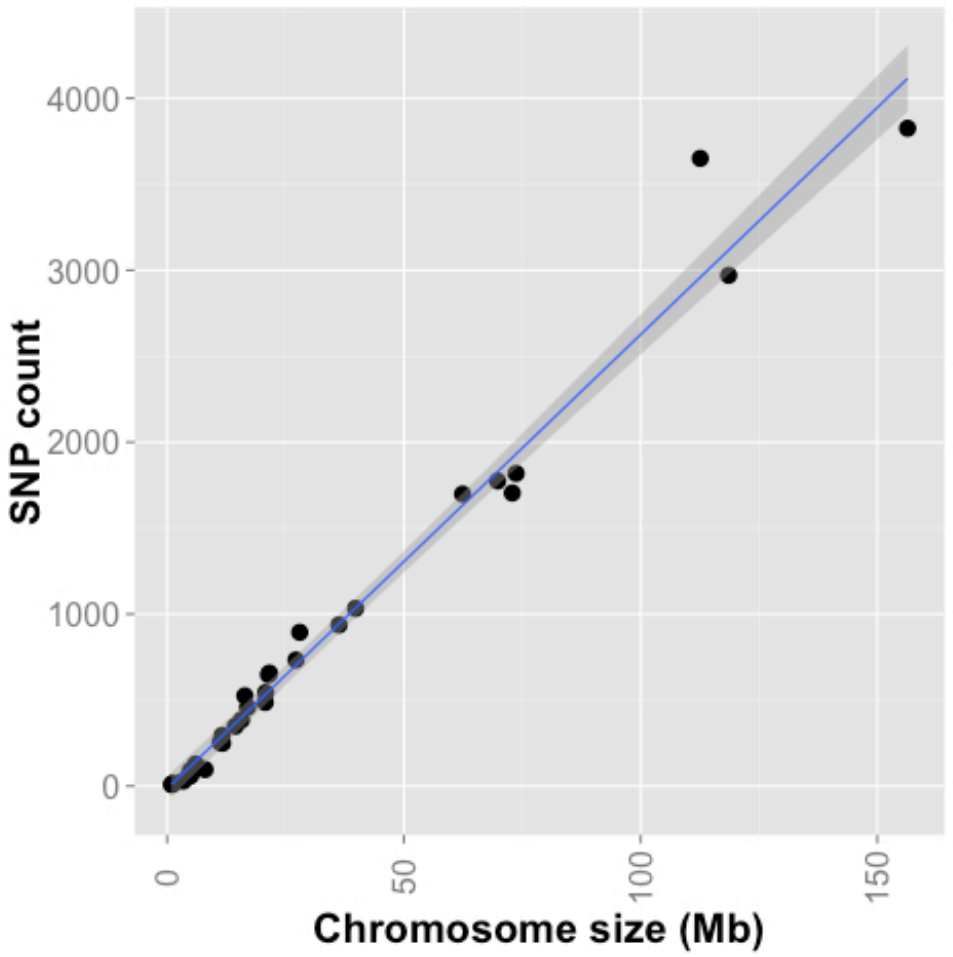

Figure S10 correlation of chromosome size and number of Single Nucleotide Polymorphisms

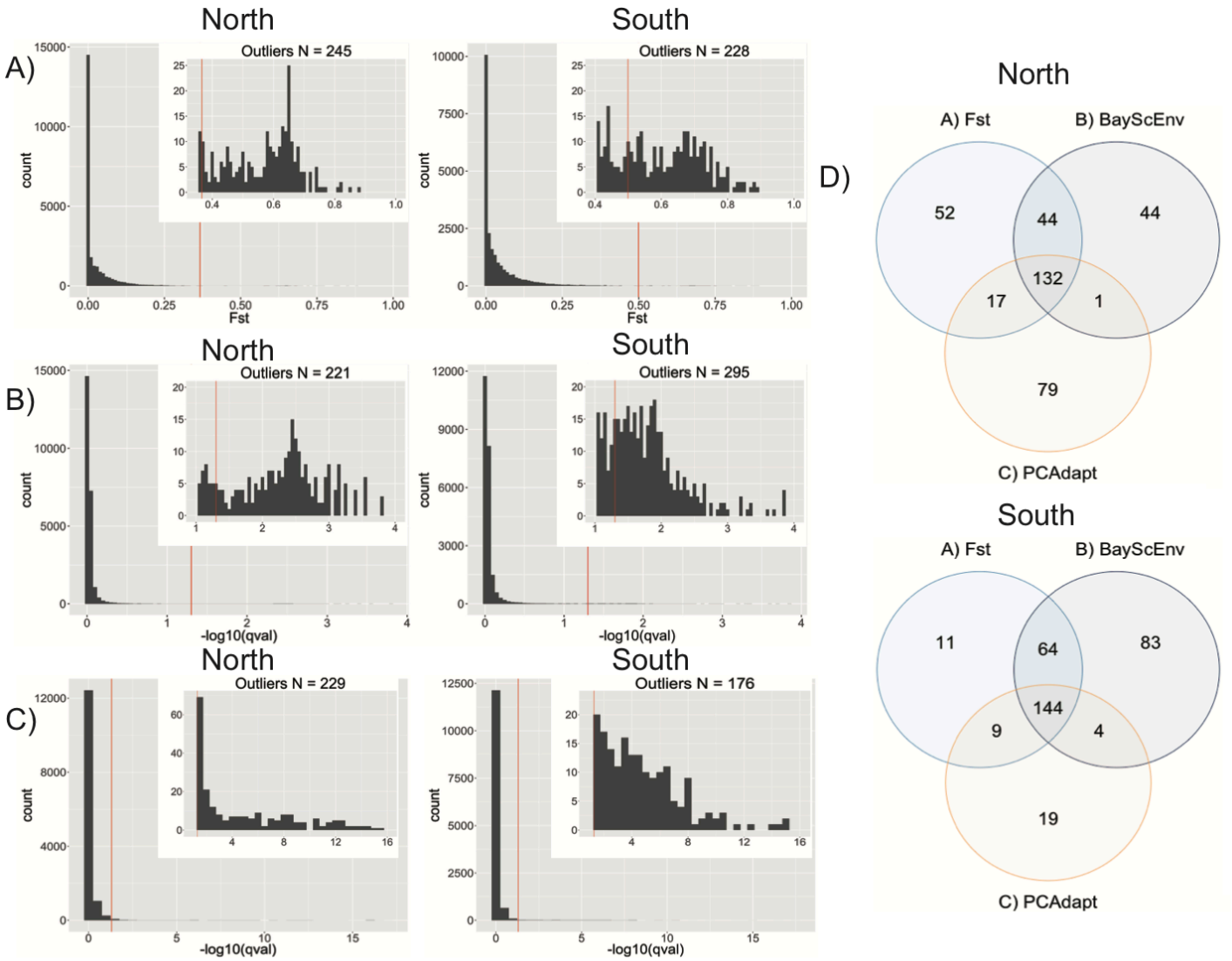

Figure S11 Results summary of outlier detection methods for unmapped loci. Histograms of distributions of various summary statistics for the different outlier detection methods employed: (A) fine-scale F_{ST} estimates (including only individuals sampled within 40 km of the centre of the contact zone), (B) BayeScEnv significance levels and (C) PCAdapt significance levels. The inset in each histogram shows the tail of the distribution. (D) Venn diagram to show the overlap of significant outliers detected between methods (A, B and C) in each transect.

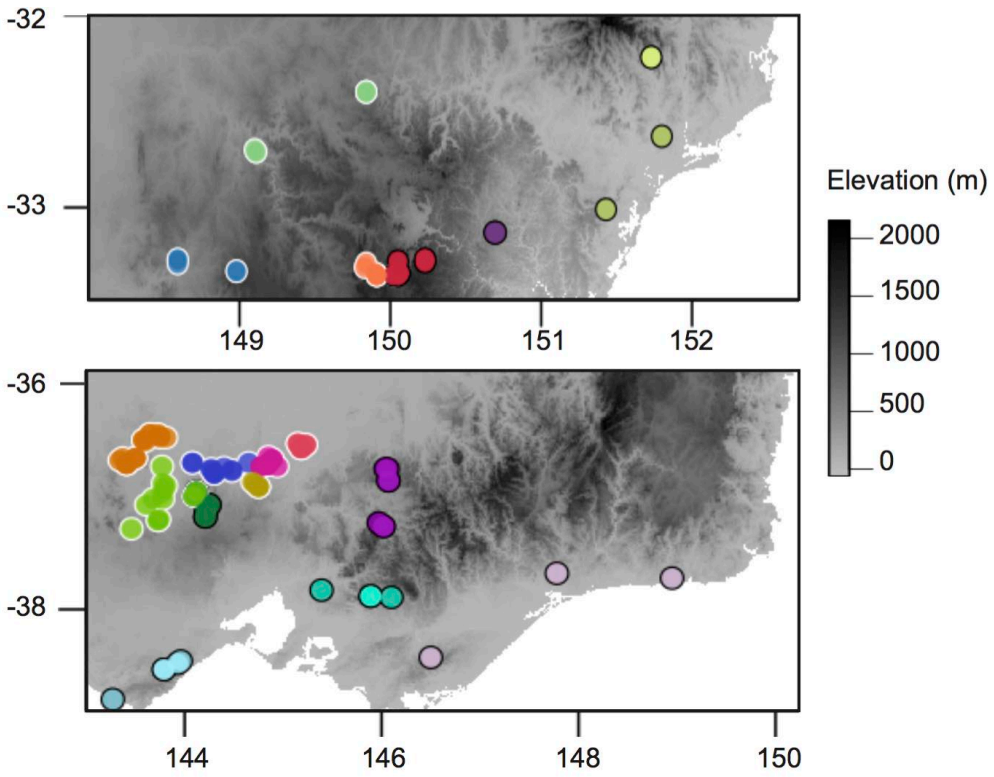

Figure S12 Populations arbitrarily defined across each transect. Samples were organized in (A) 6 populations in the north transect (mito-A = 25 individuals, mito-B = 27), and (B) 11 populations in the south transect (mito-A = 71, mito-B = 32). Each colour represents a different population Populations contain at least two individuals in close proximity and that belong to the same mitogroup.

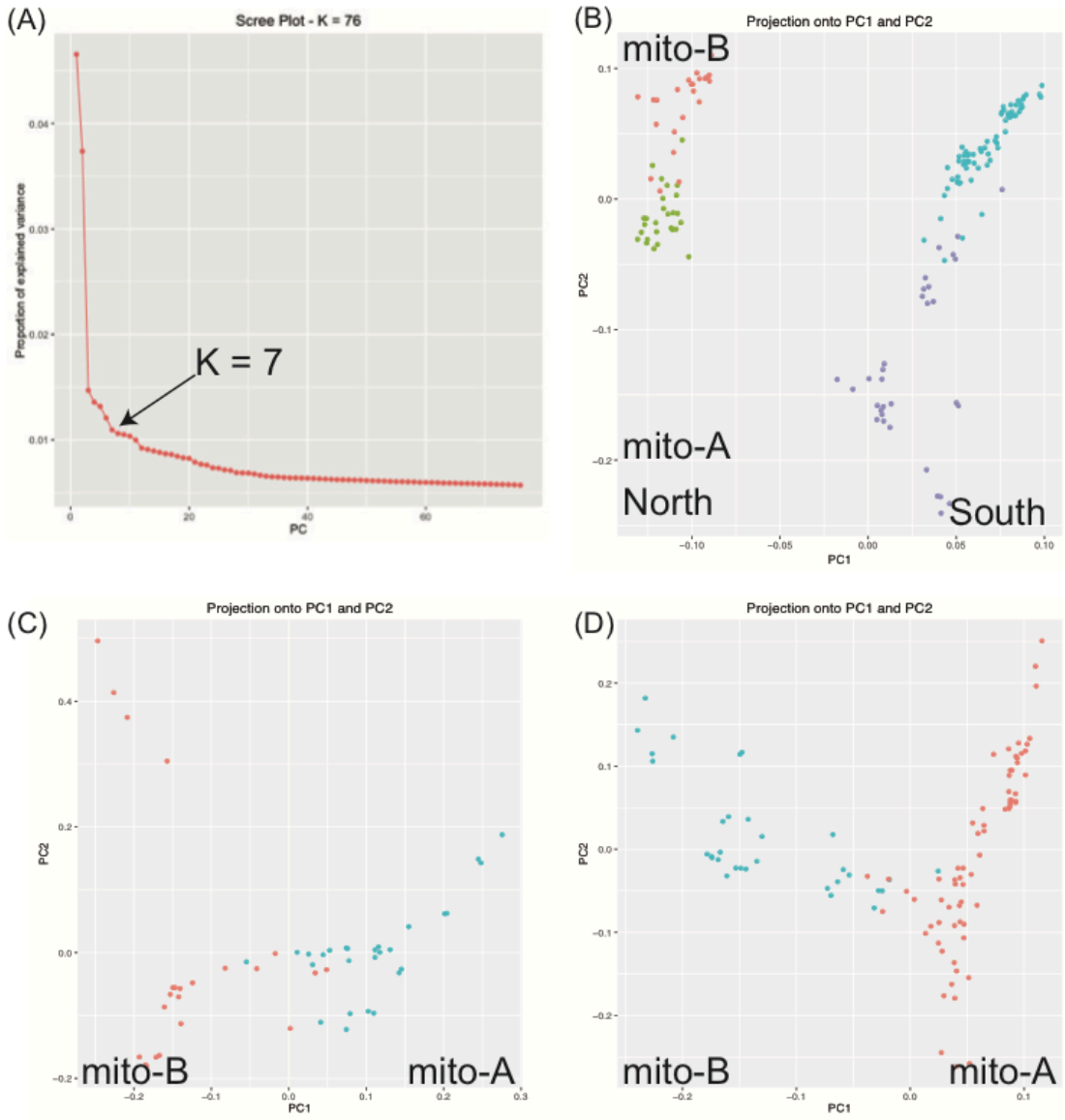

Figure S13 Summary of result for PCAdapt analyses. (A) Screeplot of the amount of genetic variation explained by the first 76 K clusters (see Methods). (B) PCA analysis of both transects (north mito-A = green, north mito-B = red, south mito-A = purple, south mito-B = blue). (C) PCA analysis of north transect (mito-A = blue, mito-B = red). (D) PCA analysis of south transect (mito-A = red, mito-B = blue).